UW-CTSM: Circular Time Shift Modulation for Underwater Acoustic Communications

Zhuoran Qi and Dario Pompili
Department of Electrical and Computer Engineering, Rutgers University-New Brunswick, NJ, USA {zhuoran.qi, pompili}@rutgers.edu

Abstract-Pulse Position Modulation (PPM) has shown great advantages by being non-coherently implementable. However, PPM suffers from the high multipath delay in underwater acoustic channels. To be robust against the effects of multipath delay and additive noise in underwater acoustic communications, this project proposes a novel modulation scheme that is nonlinear and that can be implemented non-coherently, called the Circular Time Shift Modulation (CTSM) based on the high autocorrelation property of Zero-Correlation-Zone (ZCZ) signals. The performance of CTSM in terms of bit error rate is investigated by emulations based on real underwater acoustic channels collected in the Gulf of La Spezia, Italy, using the Littoral Ocean Observatory Network (LOON) testbed hosted at the NATO Centre for Maritime Research and Experimentation (CMRE) in June 2021. The results have shown that the CTSM system has higher robustness compared with PPM in underwater acoustic communications.

Index Terms—Pulse Position Modulation, Zero-Correlation-Zone Signals, Underwater Acoustic Communications.

I. Introduction

In recent years, underwater wireless communication has played an important role in the military, commercial, and scientific fields [1]. With the increasing demand for reliable underwater wireless communication systems, three main-stream communications are considered: Underwater Radio Frequency Communication (URFC), Underwater Acoustic Communication (UAC), and Underwater Wireless Optical Communication (UWOC) [2]. The URFC provides high bandwidth and data rate [3], but radio waves suffer high attenuation in seawater due to the high conductivity and permittivity, leading to a limited coverage distance of up to a few meters. The UWOC offers a wider bandwidth in the scale of hundreds of megahertz. However, the UWOC suffers from water absorption and scattering effects and attenuates greatly. Additionally, some alignments between the transmitter and the receiver are required, and the quality of the communication link can be severely impaired by external factors, such as the presence of sources of reflection, e.g., bubbles. Different from the URFC and the UWOC, the UAC suffers less attenuation and covers a communication range of up to kilometers [4], but the underwater acoustic speed is as slow as 1500 m/s, leading to time-varying multipath delay. Moreover, the low bandwidth, sound speed variability, and frequency-dependent scattering losses [5] still make UAC a challenge.

Motivations: In UACs, Coherent Phase-Shift Keying (CPSK) modulation has been widely used, which conveys data by changing the phase of the carrier waves [6].

However, the CPSK requires a complicated demodulator to compare the phase of received signals to a reference signal. As for the linear signal with coherent detection, where the noise works on the transmitted symbols directly by introducing the phase offset, the accuracy of CPSK demodulation can be influenced dramatically. To reduce the complication of demodulation, Differential Phase-Shift Keying (DPSK) works as an alternative modulation scheme which demodulates non-coherently by measuring the phase shift of each symbol with respect to the previous symbol [7]. Nonetheless, more demodulation errors are introduced compared with CPSK because errors in the previous symbol lead to errors in the following symbols.

In contrast, the Pulse Position Modulation (PPM) is powerefficient and does not need to track the carrier phase information [8]. Instead, what we only care about is the power peak position of each received PPM frame, so that the phase offset caused by noise hardly has an impact on the PPM signal transmission and the high cost of phase detection can be discarded. In PPM modulation, data are transmitted by different pulse positions which are in proportion to the amplitude of the message signal in the time domain, while the pulse width and amplitude are the same. In this case, all of the interest information is concentrated on the peak position per PPM frame. However, PPM is sensitive to the multipath delay that arises in the underwater acoustic channel. In [9] and [10], the Rician fading channel has been shown to be a good match for the short-range shallow water channel (with a depth of less than 100 m), where the power of the Lineof-Sight (LOS) signal is stronger than the multipath delay signals. With a high Signal-to-Noise Ratio (SNR), the PPM works effectively, but with a low SNR, the power of multipath delay signals plus additive noise might be higher than that of the LOS signal, leading to demodulation errors. To improve the robustness of the UAC system at the physical layer, a non-coherent modulation scheme that can effectively defend against multipath delay and additive noise is in great need.

Proposed Approach: To solve the issues of multipath delay plus additive noise, Zero-Correlation-Zone (ZCZ) signals are utilized, whose auto-correlation function has zero-sidelobe zone. The structure of our proposed modulation is shown in Fig. 1. At the transmitter side, the data are mapped to the corresponding circular time shifts in ZCZ signals. At the receiver side, the periodic cross-correlation function between the received ZCZ signals and the initial ZCZ signal will be

calculated. The position of the peak of the periodic cross-correlation function is exactly the time shift, and the data can be demodulated successfully. The difference between the proposed approach and the PPM is that, in the proposed approach, the peak detection is done with the periodic cross-correlation between the received ZCZ signals and the initial signal, while in the PPM, the peak detection is done with the received PPM signals.

Contributions: In this work, we derive a new modulation scheme for UACs that can achieve a significant gain of several dB compared with the PPM. The contributions are as follows.

- We derive the Circular Time Shift Modulation (CTSM) including the equations of modulator and demodulator, which aims at significantly enhancing the underwater acoustic system robustness at the physical layer.
- The CTSM signal is conveyed by the non-linear modulation of circular time shifts in ZCZ signals, and the receiver does peak detection of period cross-correlation function between the received ZCZ signals and the initial ZCZ signal to recover the circular time shifts.
- The physical-layer evaluation of the proposed new modulation is carried out under a real underwater acoustic channel collected using the Littoral Ocean Observatory Network (LOON) testbed (located in the Gulf of La Spezia, Italy) hosted at the NATO Science and Technology Organization Centre for Maritime Research and Experimentation (CMRE) in June 2021. The performance includes results of Bit Error Rate (BER) with varying SNR and multipath lifetime.
- The BER and spectral efficiency performance without channel coding of PPM, Spread Spectrum-based PPM (SS-PPM) and CTSM with different channels and different modulation parameters are compared and analyzed. The physical-layer emulation results indicate that the CTSM system achieves SNR gain of several dB compared with ordinary PPM setups and a higher spectral efficiency compared with SS-PPM setups. The performance degradation caused by the multipath delay and additive noise is alleviated by the high auto-correlation of CTSM, which shows that the CTSM improves the system robustness significantly.
- The trade-off with the CTSM modulation order to balance the transmission data rate and system reliability is discussed.

This work shows that the proposal achieves higher system robustness compared with ordinary PPM and SS-PPM, albeit with an increase in computation complexity.

Paper Organization: Sect. II present the relevant publications. In Sect. III, we detail our proposed modulation scheme. In Sect. IV, we provide results from accurate emulations to evaluate the proposed modulation scheme and discuss the performance of different modulation schemes. Finally, we conclude the paper and describe the future work in Sect. V.

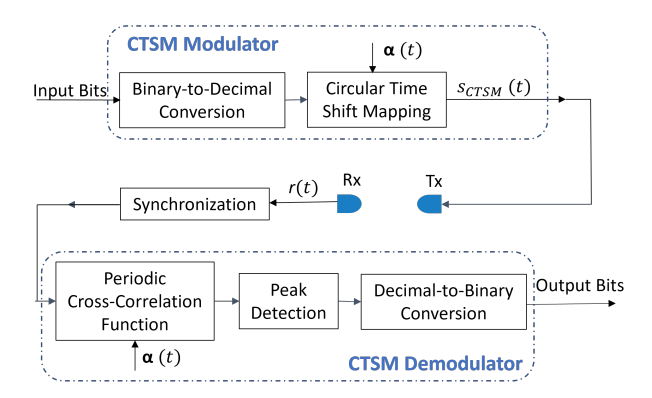


Fig. 1: Structure of our proposed UW-CTSM system, including both the speaker Tx and the hydrophone Rx; $\alpha(t)$ is the initial CTSM signal, $s_{CTSM}(t)$ is the transmitted CTSM signal, and r(t) is the received signal.

II. RELATED WORKS

Nowadays, PPM has been widely used in wireless communication systems, especially in the UWOC which has little or no multipath delay. The optimum time-shift auto-correlation is studied for time-hopping Ultra Wide Band (UWB) with PPM in [11] by calculating the relative time shift of Gaussian pulses that achieves the minimum auto-correlation with different orders. In [12], the SS-PPM using a Pseudo-Noise (PN)sequence is proposed for UACs, which calculates the crosscorrelation function of the spreading sequence and the received SS-PPM signals at the receiver and detects the peak position of the cross-correlation. The SS-PPM is more robust but presents a lower transmission rate compared with an ordinary PPM. Authors in [13] propose the Chaotic Pulse-Position and Pulse-Width Combined Modulation (CPWCM) communication system for UACs by modulating the chaotic signals with PPM and Pulse Width Modulation (PWM) alternately. The CPWCM doubles the transmission data rate of the chaotic PPM but the transmission data rate is still lower than the ordinary PPM. Different from PPM and SS-PPM, which are isochronous, i.e., the encoded symbol structure is fixed, the CPWCM is anisochronous and there is not a fixed symbol structure. When decoding CPWCM symbols, the next symbol is decoded with reference to the previous symbol, and if errors happen in previous symbols, the following symbols cannot be decoded correctly. In [14], we derive a modulation method called Orthogonal Frequency Division Multiplexing (OFDM)-PPM, which almost doubles the coverage distances in the UWOC. However, OFDM-PPM only works efficiently in the UWOC where the multipath is limited, but does not work well in the UAC which suffers high multipath delay. In this work, the system with our proposed CTSM improves the robustness in the UAC channels without sacrificing the transmission data rate compared with the ordinary PPM.

ZCZ signals have been widely used in communication systems for channel estimations and Code-Division Multiple-Access (CDMA). Authors in [15] and [16] utilize the ZCZ signals as the pilot signals and calculate the periodic cross-

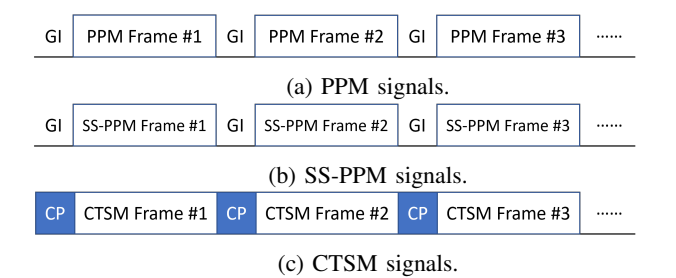


Fig. 2: Signaling structure: (a) PPM frames with zero-Guard Intervals (GIs); (b) SS-PPM frames with zero-GIs; (c) CTSM frames with Cyclic Prefix (CP).

correlation function of the received pilot signals and the transmitted pilot signals to obtain the multipath property, which shows high reliability. In [17] and [18], a ZCZ codebased Frame Start Detector (FSD) is investigated for the Multi-input Multi-output (MIMO)-OFDM system in the fast correlated Rayleigh flat fading channel. The Results show that the ZCZ code improves the FSD performance effectively by 15 %. Authors in [19] and [20] study the synchronous ZCZ-CDMA which is proved to remove the co-channel interference effectively for short-range communication. Authors in [21] and [22] study the BER performance of the synchronous optical ZCZ-CDMA with indoor experiments, which shows that ZCZ-CDMA can suppress co-channel interference with the high auto-correlation. In [23], the BER performance of the M-ary Amplitude Shift Keying Spread Spectrum (M-ary/ASK-SS) system based on the optical ZCZ code is studied in the frequency non-selective fading channel. Authors in [24] propose a method of interference-free pilot design and channel estimation by using the ZCZ sequence. In our work, we propose a novel physical-layer modulation scheme based on the auto-correlation of the ZCZ sequence, which is proved to improve the system robustness effectively compared with the ordinary PPM modulation scheme.

III. CIRCULAR TIME SHIFT MODULATION

To improve the reliability of UACs at the physical layer, we propose a new modulation scheme that enhances the robustness of the system by utilizing the high auto-correlation of ZCZ signals, called CTSM. For K-ary CTSM, first we map the original bit sequences to CTSM modulated signals by converting every $M = \log_2(K)$ bits to a decimal value which is exactly the value of the circular time shift applied to the initial CTSM signal, i.e., the ZCZ signal. The ZCZ signal is of high auto-correlation and the cross-correlation with the nonzero-time-shift signal is zero, so the periodic autocorrelation function of a ZCZ signal is an impulse function, while the periodic cross-correlation function between a ZCZ signal and a nonzero-time-shift ZCZ signal is an impulse function with the time shift. In the channel with multipath, the received time-delayed ZCZ signals can be seemed as the nonzero-time-shift signals. Therefore, the multipath information can be obtained by calculating the periodic crosscorrelation function between the received ZCZ signals and the

transmit ZCZ signal. In the Rician fading channel, which is the common model of the underwater channel, especially in the shallow water, the magnitude of the impulse response of the LOS path is always higher than that of multipath, and the signal through LOS path is usually firstly received by the receiver. If the input ZCZ signal is with a non-zero time shift, then the periodic cross-correlation function will be the channel response with the time shift. Therefore, the highest magnitude of the channel response corresponds to the time shift, and the peak detection is able to find the time shift and demodulate the signal.

Zero-Correlation-Zone Signal: Let α be the CTSM signal,

$$\alpha_k = \alpha[k] = \exp\left[\frac{2\pi\sqrt{-1}k^2}{K}\right], \ k = 0, 1, ..., K - 1,$$
 (1)

where K is the length of α . Note that the periodic auto-correlation function of α is an impulse, i.e.,

$$R_a(\boldsymbol{\alpha}) = \frac{1}{K} \boldsymbol{\alpha} A = [1, 0, \cdots, 0]^T = \delta[k], \tag{2}$$

$$A = \begin{bmatrix} \overline{\alpha_0} & \overline{\alpha_{K-1}} & \cdots & \overline{\alpha_1} \\ \overline{\alpha_1} & \overline{\alpha_0} & \cdots & \overline{\alpha_2} \\ \vdots & \vdots & \ddots & \vdots \\ \overline{\alpha_{K-1}} & \overline{\alpha_{K-2}} & \cdots & \overline{\alpha_0} \end{bmatrix}, \tag{3}$$

where $\overline{\alpha_k}$ is the complex conjugate of α_k ; "T" is a transpose of a matrix; $\delta[k]$ is an impulse signal. Since the auto-correlation function of α has zero-sidelobe zone, α is called a ZCZ signal.

CTSM Modulator: We consider K-ary CTSM modulation, in which $M = \log_2(K)$ message bits are encoded by the CTSM signal with a length of K in each frame. Let $\boldsymbol{x_n}$ be the transmit signal,

$$x_n = \alpha \circledast \delta[k - n], \tag{4}$$

$$x_n[k] = \alpha[\langle k - n \rangle_K], \quad n = 0, 1, ..., K - 1, k = 0, 1, ..., K - 1,$$
 (5)

where " \circledast " denotes a circular convolution, $x_0 = \alpha$, $\alpha < k - n >_K$] represents a circular shift of α by n samples to the right. Each circular time shift contains a different message which are modulated bits. For example, when the modulation order K = 16, a $M = \log_2(K) = 4$ -bit sequence "1001" corresponds to the 16-ary CTSM signal $x_9[k] = \alpha < k - 9 >_{16}$. When we calculate the periodic cross-correlation function between x_n and α , we get,

$$R_{c}(\boldsymbol{x}_{n},\boldsymbol{\alpha}) = \frac{1}{K}\boldsymbol{x}_{n}A = \frac{1}{K}\boldsymbol{\alpha} \circledast \delta[k-n]A$$

$$= \frac{1}{K}\boldsymbol{\alpha}A \circledast \delta[k-n] = \delta[k] \circledast \delta[k-n], \quad (6)$$

$$= \delta[k-n], \quad n = 0, 1, ..., K-1.$$

CTSM Demodulator: Assume that there is only one hydrophone at the receiver, the transmit signal $\boldsymbol{x_n}$ is through the channel with a response $\mathbf{h} = [h_0, h_1, h_2, ...]$, the received CTSM signals $\hat{\boldsymbol{y}_n}$ can be expressed as,

$$\hat{\mathbf{y}}_{n} = \mathbf{x}_{n} * \mathbf{h},\tag{7}$$

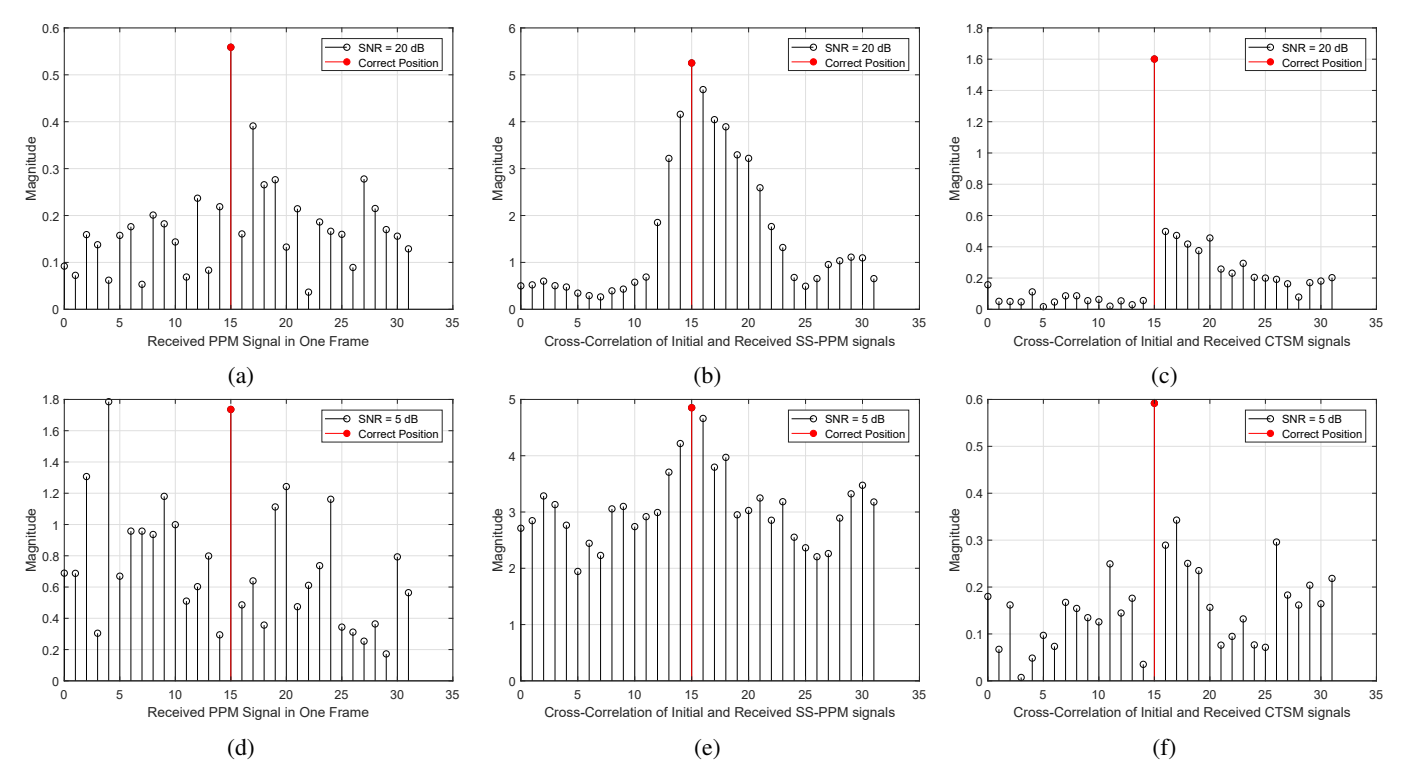


Fig. 3: When the multipath lifetime is 3.13 ms, the CTSM time shift or the PPM pulse position is 15, with an SNR of 20 dB, (a) received PPM signal in one frame; (b) cross-correlation of the received SS-PPM signal and initial spreading sequence; (c) periodic cross-correlation of the received CTSM signal and the initial CTSM signal. When the SNR is 5 dB, (d) received PPM signal in one frame; (e) cross-correlation of the received SS-PPM signal and initial spreading sequence; (f) periodic cross-correlation of the received CTSM signal and initial CTSM signal.

where "*" denotes a convolution. To reduce the Inter-Symbol Interference (ISI), a Cyclic Prefix (CP) with a length of L is added, $L \leq K$. Assume \hat{L} is the maximum multipath delay in the time-discrete model. When $L \geq \hat{L}$, the channel reverberation is correctable. There is a relationship between the CP-removed sequence y_n , the input sequence x_n , and the channel response \mathbf{h} , as follows,

$$egin{aligned} oldsymbol{y_n} &= oldsymbol{x_n} \circledast oldsymbol{\mathsf{h}} \ &= oldsymbol{x_n} \left[egin{array}{cccc} h_0 & h_1 & \cdots & h_{K-1} \ h_{K-1} & h_0 & \cdots & h_{K-2} \ dots & dots & \ddots & dots \ h_1 & h_2 & \cdots & h_0 \end{array}
ight]. \end{aligned}$$

If α is shared by the transmitter as well as the receiver, the channel impulse response can be obtained by calculating the periodic cross-correlation function between y_n and α ,

$$R_{c}(\mathbf{y}_{n}, \boldsymbol{\alpha}) = \frac{1}{K} \mathbf{y}_{n} A = \frac{1}{K} \mathbf{x}_{n} \circledast \mathbf{h} A$$

$$= \frac{1}{K} \mathbf{x}_{n} A \circledast \mathbf{h} = \delta[k - n] \circledast \mathbf{h}$$

$$= \mathbf{h}[\langle k - n \rangle_{K}], \quad n = 0, 1, ..., K - 1.$$
(9)

In the UACs, the channel model is usually the Rician fading channel, where the magnitude of the LOS path impulse h_0 should be the highest among $[h_0, h_1, h_2, ...]$. Therefore, the

receiver only needs to do the peak detection after calculating $R_c(y_n, \alpha)$. The position of the peak is the circular shift n.

IV. PERFORMANCE EVALUATION

In this section, we go further on the physical-layer emulator of our proposed CTSM system by introducing its parameters in detail. To emphasize the performance of the modulation schemes, we present the emulation results of the BER and the spectral efficiency without channel coding. The performance of the Reed–Solomon (RS)-coded BER with different code rates is also presented. Note that emulations are based on the real UAC channels with a depth of 10 m and a distance range of about 100 m collected by the CMRE LOON testbed in the Gulf of La Spezia, Italy, in June 2021. The emulation results with 95% confidence intervals are provided to ensure statistical relevance of the emulation results.

System Model: The structure of our proposed CTSM system is shown in Fig. 1. At the transmitter, we first convert the binary bits to decimal values. Given the modulation order of K, every $M = \log_2(K)$ bits are converted to a decimal value, and the decimal value is applied to the circular time shift of the initial CTSM signal. There will be K values of circular time shifts in total, from 0 to K-1. Then the CTSM signal $s_{CTSM}(t)$ is transmitted by the transmitter and received by the receiver. At the receiver, the time synchronization is done prior

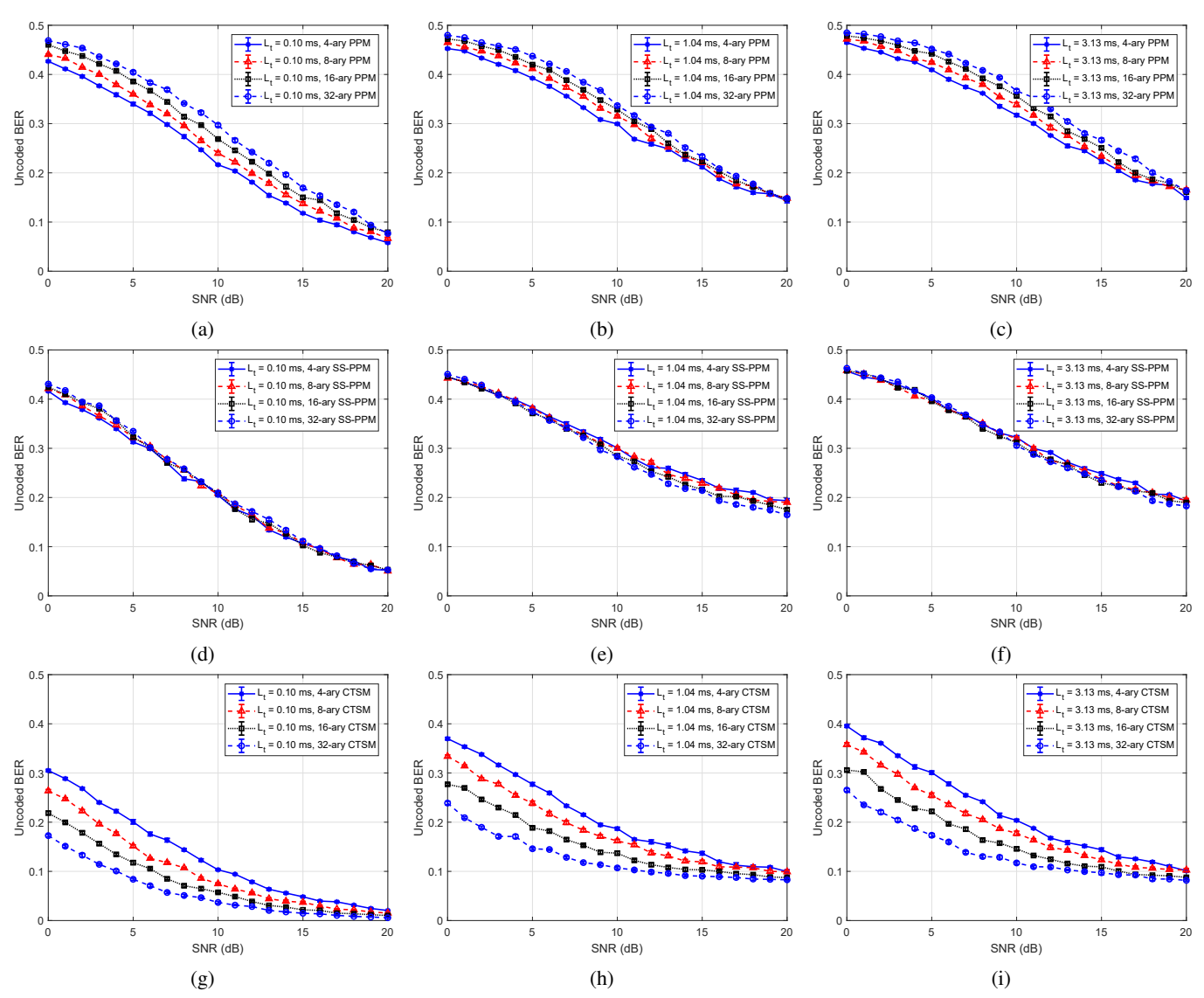


Fig. 4: L_t represents the multipath lifetime. The uncoded BER of PPM with different values of multipath lifetime and 95% confidence intervals: (a) $L_t=0.10$ ms; (b) $L_t=1.04$ ms; (c) $L_t=3.13$ ms. The uncoded BER of SS-PPM with different values of multipath lifetime and 95% confidence intervals: (d) $L_t=0.10$ ms; (e) $L_t=1.04$ ms; (f) $L_t=3.13$ ms. The uncoded BER of CTSM with different values of multipath lifetime and 95% confidence intervals: (g) $L_t=0.10$ ms; (h) $L_t=1.04$ ms; (i) $L_t=3.13$ ms. Note that the confidence intervals are <0.01 and hence are not visible in the figures.

TABLE I: Parameters Setting for Emulations.

Parameter	Value
DAC sampling rate	48 kHz
Symbol rate	6 kBd
Frequency band of LOON testbed	8-14 kHz
Bandwidth of LOON testbed	$6~\mathrm{kHz}$
ADC sampling rate	$128~\mathrm{kHz}$
Source modulation	PPM, SS-PPM or CTSM
Modulation order K	4, 8, 16, 32
Carrier frequency f_c	11 kHz
Number of speakers	1
Number of hydrophones	1
Sound power level re 1 pW	180 dB
CP/GI length	0.21 ms

to CTSM demodulation. The periodic cross-correlation function calculation between the received CTSM signals and the initial CTSM signal and the peak detection are subsequently performed. The position of the peak corresponds to the circular time shift. With the decimal to binary conversion, the received signals are demodulated. The transmit signal structures of PPM, SS-PPM and CTSM are shown in Fig. 2, where the PPM/SS-PPM utilizes zero-Guard Intervals (GIs) to reduce the ISI, and the CTSM utilizes CP to reduce the ISI.

Parameters for the emulator are in Table I. At the transmitter, we employ a carrier frequency of $f_c=11~\mathrm{kHz}$. There is only one speaker and one hydrophone whose locations are fixed. The modulation order in the PPM/SS-PPM/CTSM

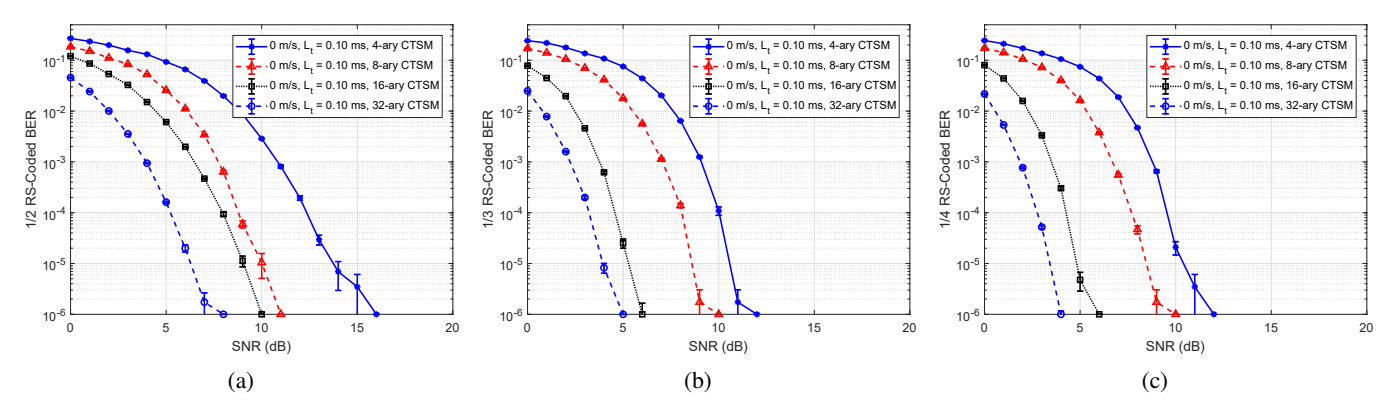


Fig. 5: L_t represents the multipath lifetime. The RS-coded BER of CTSM with (a) 1/2 code rate; (b) 1/3 code rate; (c) 1/4 code rate and with 95% confidence intervals when $L_t = 0.10$ ms.

frame is chosen to be 4, 8, 16, 32, so that the reliability with different modulation schemes can be observed. To compare the modulations fairly, we perform signal equalization so that the power values of different modulations with different orders are equal. The frequency band is $8-14~\mathrm{kHz}$ so the bandwidth is limited to $6~\mathrm{kHz}$. The sampling rate of the Digital-to-Analog Converter (DAC) is up to $48~\mathrm{kHz}$ and the sampling rate of the Analog-to-Digital Converter (ADC) is up to $128~\mathrm{kHz}$. The sound power level re $1~\mathrm{pW}$ is $180~\mathrm{dB}$. The length of CP/GI is set as $0.21~\mathrm{ms}$. The additive noise is assumed to be the Additive White Gaussian Noise (AWGN).

Results and Findings: The major findings of the following emulation results include system robustness enhancement when in channels with multipath delay and additive noise and the SNR gain measured by the uncoded BER. In Fig. 3. which is based on the ordinary PPM, the SS-PPM [12] with a spreading length of 4, and the CTSM, it is found that the system robustness in the channel with multipath and additive noise is improved significantly by CTSM. To observe the performance of PPM/SS-PPM/CTSM with different levels of SNR, we fix the multipath delay with a lifetime of 3.13 ms. Figs. 3(a) and 3(d) depict the received PPM signal and the peak detection. Figs. 3(b) and 3(e) depict the cross-correlation function between the received SS-PPM signals and the initial spreading sequence. Figs. 3(c) and 3(f) depict the periodic cross-correlation function between the received CTSM signals and the initial CTSM signal, i.e., $R_c(y_n, \alpha)$ in (9). When the SNR is 20 dB, it can be observed that the peak detection works effectively in PPM/SS-PPM/CTSM, where the pulse positions and the correct circular time shift can be found and the received signals can be demodulated successfully. When the SNR is 5 dB, the peak detection still works with the SS-PPM/CTSM and the SS-PPM/CTSM signals can be demodulated correctly. However, for the PPM, due to the combined effects of the multipath delay and the additive noise, the peak of the received PPM signal is no longer at the correct pulse position. Therefore, errors occur in the PPM demodulation. Moreover, it is obvious that the interference in the periodic cross-correlation of the received CTSM is much less than that in the cross-correlation of the received SS-PPM.

Fig. 4 depicts uncoded BER performance of the PPM/SS-PPM/CTSM with different channel conditions. The SNR varies from 0 to 20 dB. The uncoded BER performance of the PPM with the increasing of the modulation order is shown in Figs. 4(a-c). The uncoded BER performance of the SS-PPM is similar with different modulation orders, and is slightly lower than the uncoded BER of the 4-ary PPM. The performance of CTSM is depicted in Figs. 4(g-i), where we can observe that the uncoded BER of CTSM is much lower than that of PPM/SS-PPM. In addition, the uncoded BER performance of CTSM with a higher modulation order is better than that with a lower modulation order. The reason why it performs like that is that with a higher modulation order, the ZCZ signal is longer, which leads to a higher auto-correlation and increases the accuracy of peak detection. Given the CP length is 0.21 ms. the uncoded BER of 32-ary CTSM reaches 0 when the SNR is 20 dB, as shown in Fig. 4(g). However, when the multipath lifetime is longer than the CP length, as shown in Figs. 4(h) and 4(i), the uncoded BER increases dramatically because the auto-correlation of the CTSM is damaged by the multipath delay. When the multipath lifetime is 0.10 ms, the uncoded BER of 4-ary CTSM is lower than 0.1 when the SNR is higher than 10 dB, and the uncoded BER of 4-ary PPM is lower than 0.1 when the SNR is higher than 16 dB. The uncoded BER of 32-ary CTSM is lower than 0.1 when the SNR is higher than 4 dB, and the uncoded BER of 32-ary PPM is lower than 0.1 when the SNR is higher than 19 dB. Comparing the uncoded BER performance versus SNR of CTSM and PPM, we can find that the CTSM reaches an SNR gain of more than 6 dB. When channel coding is applied, the BER of the CTSM is reduced. Fig. 5 depicts the BER of the CTSM with different channel coding rates of RS coding, which shows that with channel coding, the BER of 32-ary CTSM can reach as low as 10^{-6} when SNR is 4 dB with 1/4 RS code rate, which meets most users' demand. In Fig. 5(a), The 4-ary CTSM reaches 10^{-6} when the SNR is higher than 16 dB, while the 32-ary CTSM reaches 10^{-6} when the SNR is higher than $8~\mathrm{dB}$ which achieves an SNR gain of 8 dB.

Fig. 6 depicts the uncoded spectral efficiency performance of systems with the PPM/SS-PPM/CTSM, the bandwidth is

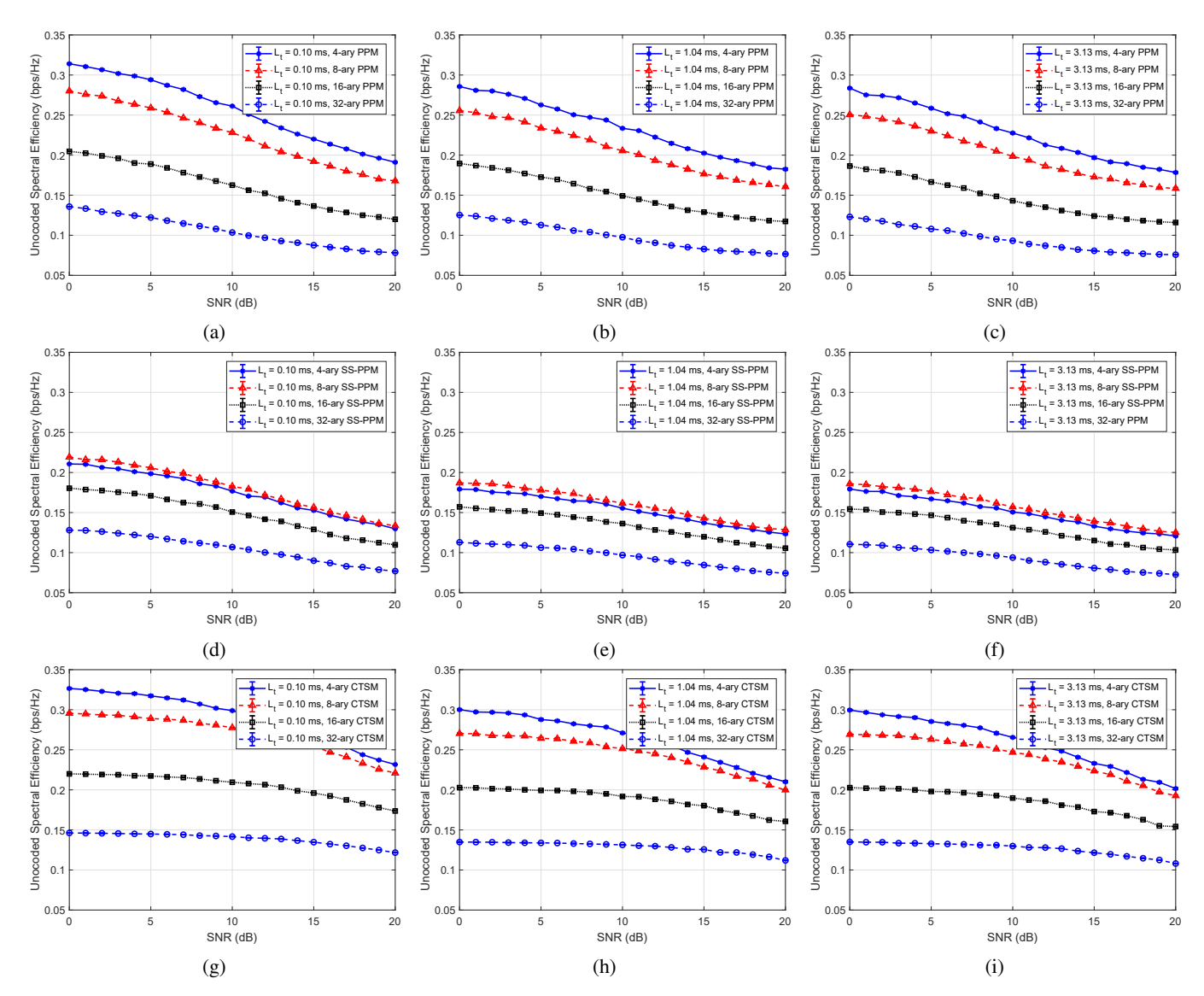


Fig. 6: L_t represents the multipath lifetime. With a bandwidth of 6 kHz, the uncoded spectral efficiency of PPM with different values of multipath lifetime and 95% confidence intervals: (a) $L_t=0.10~\rm ms$; (b) $L_t=1.04~\rm ms$; (c) $L_t=3.13~\rm ms$. The uncoded spectral efficiency of SS-PPM with different values of multipath lifetime and 95% confidence intervals: (d) $L_t=0.10~\rm ms$; (e) $L_t=1.04~\rm ms$; (f) $L_t=3.13~\rm ms$. The uncoded spectral efficiency of CTSM with different values of multipath lifetime and 95% confidence intervals: (g) $L_t=0.10~\rm ms$; (h) $L_t=1.04~\rm ms$; (i) $L_t=3.13~\rm ms$. The confidence intervals are close to 10^{-3} and hence are not visible in the figures.

6 kHz. The uncoded spectral efficiency η is calculated as follows [12],

$$\eta = \begin{cases}
\frac{f_s \times \log_2(K)}{B_w(L+K)} (1-\epsilon), & \text{for PPM/CTSM,} \\
\frac{f_s \times \log_2(K)}{B_w(L+K+L_s-1)} (1-\epsilon), & \text{for SS-PPM,}
\end{cases}$$
(10)

where f_s is the symbol rate in Bd; B_w is the bandwidth; K is the modulation order; L is the length of the CP in the time-discrete model; L_s is the spreading length of the SS-PPM; ϵ is the uncoded BER. It can be observed from Fig. 6 that the uncoded spectral efficiency of the CTSM is higher than that of the PPM, since the uncoded BER of the CTSM is much lower than that of the PPM. The spectral efficiency of SS-PPM is lower than for PPM/CTSM, because SS-PPM

introduces the spreading sequence. Moreover, with a higherorder modulation, the uncoded spectral efficiency of CTSM decreases dramatically. Therefore, there is a trade-off between the BER and spectral efficiency. When the low BER is in demand, the higher modulation order is considered. When the high spectral efficiency is in demand, the lower modulation order is considered.

V. CONCLUSION AND FUTURE WORK

We proposed a novel physical-layer modulation scheme for UnderWater (UW) acoustic communications, called Circular Time Shift Modulation (UW-CTSM), to improve system robustness when in underwater acoustic channels affected by multipath and additive noise. The key feature of the proposed modulation is the utilization of the high auto-correlation of Zero-Correlation-Zone (ZCZ) signals. The UW-CTSM was further validated under emulations using real underwater acoustic channels. Results indicated that the proposed CTSM modulation reaches a Signal-to-Noise Ratio (SNR) gain of several dB compared with the ordinary PPM and SS-PPM modulation schemes. The trade-off between Bit Error Rate (BER) and uncoded spectral efficiency was also discussed.

Notice that our UW-CTSM has a low transmission data rate as well as a low spectral efficiency. The next goal is to improve the transmission data rate and the spectral efficiency in underwater acoustic communications. Moreover, the CTSM performance versus different Doppler frequency shifts will be thoroughly studied. Simulations with different channel models and real-time experiments based on Software-Defined Radio (SDR) testbed will be designed and performed. Performance in terms of BER and spectral efficiency versus different scenarios will be analyzed.

Acknowledgement: This work was supported by the NSF NeTS Award No. CNS-1763964. The authors would like to thank Rutgers graduate students A. Jesuraj and V. Desai for helping out with the emulations.

REFERENCES

- [1] M. Ali, D. N. Jayakody, T. Perera, A. Sharma, K. Srinivasan, and I. Krikidis, "Underwater communications: Recent advances," 2019, pp. 1-10.
- [2] H. Kaushal and G. Kaddoum, "Underwater optical wireless communication," in IEEE Access, vol. 4, 2016, pp. 1518–1547.
- [3] M. Soomro, S. N. Azar, O. Gurbuz, and A. Onat, "Work-inprogress: Networked control of autonomous underwater vehicles with acoustic and radio frequency hybrid communication," in IEEE Real-Time Systems Symposium (RTSS), 2017, pp. 366-
- [4] A. Rodionov, S. Kulik, F. Dubrovin, and P. Unru, "Experimental estimation of the ranging accuracy using underwater acoustic modems in the frequency band of 12 kHz," in The 27th Saint Petersburg International Conference on Integrated Navigation Systems (ICINS), 2020, pp. 1–3.
- [5] D. Pompili, T. Melodia, and I. F. Akyildiz, "Three-dimensional and two-dimensional deployment analysis for underwater acoustic sensor networks," in Ad Hoc Networks, vol. 7, no. 4, 2009, pp. 778 – 790.
- [6] L. Jiang-Qiao, S. Anwar, Z. Xiao-Liang, G. Yun, S. Hai-Xin, and Q. Jie, "Autocorrelation based modulation recognition of PSK signals for OFDM in underwater acoustics communication," in The 15th International Bhurban Conference on Applied Sciences and Technology (IBCAST), 2018, pp. 751-756.
- [7] A. Z. M. Imran, M. M. Hossen, and M. T. Islam, "Capacity optimization of underwater acoustic communication system," in The 3rd International Conference on Electrical Engineering and Information Communication Technology (ICEEICT), 2016, pp.
- [8] H. Sari and B. Woodward, "Underwater acoustic voice communications using digital pulse position modulation," in Oceans '97. MTS/IEEE Conference Proceedings, vol. 2, 1997, pp. 870-
- [9] A. Radosevic, J. G. Proakis, and M. Stojanovic, "Statistical characterization and capacity of shallow water acoustic channels," in *OCEANS 2009-EUROPE*, 2009, pp. 1–8. [10] H. Kulhandjian and T. Melodia, "Modeling underwater acous-
- tic channels in short-range shallow water environments," in

- Proceedings of the International Conference on Underwater Networks & Systems, 2014, pp. 1-5.
- [11] J. George, S. Shaaban, and K. El Shennawy, "Optimum time shift autocorrelation for time hopping UWB system using PPM technique," in National Radio Science Conference, 2007, pp. 1–6.
- [12] G. Zhang, J. M. Hovem, H. Dong, S. Zhou, and S. Du, "An efficient spread spectrum pulse position modulation scheme for point-to-point underwater acoustic communication," Applied Acoustics, vol. 71, no. 1, pp. 11-16, 2010.
- [13] L. Zhang, J. Wang, J. Tao, and S. Liu, "A new pulse modulation method for underwater acoustic communication combined with multiple pulse characteristics," in IEEE International Conference on Signal Processing, Communications and Computing (ICSPCC), 2018, pp. 1–6.
- [14] Z. Qi, X. Zhao, and D. Pompili, "Range-extending optical transceiver structure for underwater vehicles and robotics," in Proceedings of the International Conference on Underwater Networks & Systems, ser. WUWNET'19. New York, NY, USA: Association for Computing Machinery, 2019.
- [15] N. Suehiro, R. Jin, C. Han, and T. Hashimoto, "Performance of very efficient wireless frequency usage system using kronecker product with rows of DFT matrix," in IEEE Information Theory Workshop - ITW '06 Chengdu, 2006, pp. 526-529.
- T. Ebihara and K. Mizutani, "Underwater acoustic communication with an orthogonal signal division multiplexing scheme in doubly spread channels," in IEEE Journal of Oceanic Engineering, vol. 39, no. 1, 2014, pp. 47-58.
- [17] A. K. Samingan, M. Syed, S. Abdul Rahman, N. Mohamad Anas, and S. Thiagarajah, "Zero correlation zone (ZCZ) code assisted frame start detector with combining strategy for 2x2 MIMO-OFDM systems," in IEEE International Conference on Telecommunications and Malaysia International Conference on Communications, 2007, pp. 500-504.
- [18] A. K. Samingan, M. Syed, S. Abdul Rahman, N. Mohamad Anas, and S. Thiagarajah, "Triggering strategy for zero correlation zone (ZCZ) code assisted frame start detector for 2x2 MIMO-OFDM systems," in IEEE International Conference on Telecommunications and Malaysia International Conference on Communications, 2007, pp. 505-509.
- J. Huang, S. Matsufuji, T. Matsumoto, and N. Kuroyanagi, "A study on ZCZ-CDMA systems in short-range wireless communications," in IEEE 9th Malaysia International Conference on Communications (MICC), 2009, pp. 565-569.
- [20] J. Huang, S. Matsufuji, T. Matsumoto, N. Kuroyanagi, and P. Fan, "On BFSK-ZCZ-CDMA systems," in The 4th International Workshop on Signal Design and its Applications in Communications, 2009, pp. 32-35.
- [21] T. Matsumoto, Y. Suwaki, and S. Matsufuji, "Indoor experiment of BER performance of optical CDMA system using optical ZCZ code," in The 12th International Conference on Advanced Communication Technology (ICACT), vol. 1, 2010, pp. 890–893.
- [22] T. Matsumoto, M. Kurashita, Y. Ohira, H. Torii, Y. Ida, and S. Matsufuji, "Influence of ISI on synchronous OCDMA system using an optical ZCZ sequence set on a diffuse channel," in The 8th International Workshop on Signal Design and Its Applications in Communications (IWSDA), 2017, pp. 159–163.
- [23] T. Matsumoto and S. Matsufuji, "BER performance of Mary/ASK-SS system using compact matched filter bank for optical ZCZ code," in The 12th International Conference on Advanced Communication Technology (ICACT), vol. 1, 2010, pp. 617-622.
- [24] H. Chen, R. Zhang, W. Zhai, X. Liang, and G. Song, "Interference-free pilot design and channel estimation using ZCZ sequences for MIMO-OFDM-based C-V2X communications," in China Communications, vol. 15, no. 7, 2018, pp. 47– 54.